High-resolution time-delay estimation and filter identification methods with an application to ultrasound non-destructive testing

Méthodes d'estimation de temps de retard à haute résolution et d'identification de filtre - Application au contrôle non destructif ultrasonore

Y. Deville (1), A. Talon (1)(2), E. Juliac (2)

(1) Laboratoire d'Astrophysique de Toulouse-Tarbes, Observatoire Midi-Pyrénées - Université Paul Sabatier, 14 Av. Edouard Belin, 31400 Toulouse, France.
(2) Turbomeca, 64511 Bordes Cedex, France.
ydeville@ast.obs-mip.fr , arnaud.talon@turbomeca.fr , etienne.juliac@turbomeca.fr

Abstract: Ultrasound signals involved in non-destructive testing (NDT) typically consist of two echos which have the same waveform up to a time delay and a scale factor, or more generally up to a filter. NDT then requires to estimate this delay or filter. We show that this may be achieved by resp. using high-resolution time-delay estimation methods and a frequency-domain FIR filter identication technique. The good performance of these approaches is demonstrated by means of various experimental tests, using e.g. polystyrene and Titanium Aluminide (TiAl) samples.

Résumé: Les signaux ultrasonores mis en jeu dans le domaine du Contrôle Non Destructif (CND) sont typiquement constitués de deux échos qui ont la même forme à un retard temporel et un facteur d'échelle près, ou plus généralement à un filtre près. Le CND nécessite alors d'estimer ce retard ou ce filtre. Nous montrons que cela peut être réalisé en utilisant resp. des méthodes d'estimation de temps de retard à haute résolution et une technique d'identification de filtre RIF opérant dans le domaine fréquentiel. Les bonnes performances de ces approches sont prouvées à l'aide de divers tests expérimentaux, utilisant par exemple des échantillons de polystyrène et d'aluminures de titane (TiAl).

1 Problem statement

Ultrasound non-destructive testing (NDT) aims at analyzing the defects in a material sample. To this end, an acoustic pulse is applied to the considered sample and its response is measured by a transducer, which thus provides a so-called A-SCAN signal. This signal typically consists of a series of echos, corresponding to the reflections of the emitted pulse on the front side of the sample, on the defects that it contains if any, and possibly on the back side of the sample. Analyzing the presence, time delays and shapes of these echos respectively make it possible to detect the existence of defects, to estimate their positions (i.e. their depths in the sample) and to characterize them. Although these principles may be defined in a simple way, practical application of classical NDT methods, such as Hilbert transform based techniques or cepstral analysis, often yields limited performance, due e.g. to the sensitivity of these methods to noise.

In Section 2, we first analyze how high-resolution methods, which have mainly been developed for array processing problems and spectral analysis, may be adapted to time-delay estimation (TDE). The latter problem is faced in ultrasound NDT applications when only considering simple propagation/diffraction phenomena: the basic model for the A-SCAN signal $s(n)$ reads

$$s(n) = w(n) + aw(n - n_0) \tag{1}$$

where $w(n)$ is the signal reflected by the front side of the analyzed material sample and $aw(n - n_0)$ is the signal reflected by the defect: this basic model assumes that a single defect exists and that the reflected signal that it yields is an attenuated and time-delayed version of the signal reflected by the front side. In Section 3, we then consider a more complex model, where the signal reflected by the defect is a filtered version of the waveform $w(n)$ associated to front side reflection, so that

$$s(n) = w(n) + w(n) * h(n) \tag{2}$$

where $h(n)$ is the impulse response associated to the defect. We then describe a frequency-domain method which makes it possible to estimate $h(n)$. The application of both types of methods to NDT is presented in Section 4, together with corresponding conclusions.

2 High-resolution time-delay estimation methods

As stated above, high-resolution methods, such as the *minimum variance* approach (also referred to as Capon's method) and *MUSIC*, have especially been investigated in two domains. Several of them were initially introduced in the frame of *array signal processing* [1]-[3]. In that case, a set of sensors provide signals typically resulting from the propagation of plane waves (e.g. associated to an acoustic or electromagnetic field), with additive noise. These methods then especially aim at estimating:

- the angles which define the directions of propagation of the considered waves, thus making it possible to localize the sources which emit these waves,
- or the frequency-wavenumber power spectral density associated to the considered field.

High-resolution methods were also applied to the *spectral analysis* of a single signal [4],[5]. This signal may be a sum of complex sinusoids and of complex noise, and one may then aim at estimating unknown parameters of these sinusoids. More generally, one may consider a wide-sense stationary random process and estimate its power spectral density.

We now summarize the principles of two popular high-resolution spectral analysis methods, because we will then show that they have a direct relationship with the problem that we address in this paper. The minimum variance (MV) method provides an estimate of the (non-normalized) power spectral density, defined at normalized frequency f as [4],[5]

$$\hat{P}_{MV}(f) = \frac{1}{e^H \hat{R}_{xx}^{-1} e} \tag{3}$$

where $\hat{R}_{xx}$ is the estimated autocorrelation matrix of the analyzed signal $x(n)$, ^{H} stands for complex conjugate transpose and

$$e = [1 \quad exp\ (j2\pi f) \quad \dots \quad exp\ (j2\pi(L-1)f)]^T \tag{4}$$

where L is the order the optimum FIR filters associated to this approach and ^{T} denotes transpose. If the considered signal $x(n)$ consists of a sum of complex sinusoids with unknown frequencies f_i and of noise, one may therefore try to estimate these parameters f_i as the frequencies f where the spectral estimator $\hat{P}_{MV}(f)$ defined in (3) has maxima. Indeed, for a single complex sinusoid with frequency f_1 and complex white noise, the peak of $P_{MV}(f)$ occurs at $f = f_1$ [4]. However, even with only two complex sinusoids in white noise, in general the peaks of $P_{MV}(f)$ are not situated exactly at the frequencies of these sinusoids [4].

Similarly, for a signal $x(n)$ consisting of a sum of Q complex sinusoids with unknown frequencies f_i and of complex white noise, the MUSIC method [4] estimates the frequencies f_i as the Q largest peaks of

$$\hat{P}_{MUSIC}(f) = \frac{1}{\sum_{i=Q+1}^{L} |e^H \hat{v}_i|^2} \tag{5}$$

where e is again defined by (4) and $\hat{v}_i$ with $i = 1 \dots L$ are the eigenvectors, corresponding to the eigenvalues in decreasing order, of the $L * L$ estimated autocorrelation matrix $\hat{R}_{xx}$ of the analyzed signal $x(n)$.

Now consider the TDE problem, which corresponds to our goal in this paper. For the sake of generality, we here start with an extended signal model, as compared to the single-defect NDT model (1) that we eventually aim at analyzing in the first part of this paper: we assume that the available signal $s(n)$ is a sum of Q scaled and time-delayed versions of the same waveform, with additive noise $u(n)$, i.e

$$s(n) = w(n) + \sum_{i=2}^{Q} a_i w(n - n_i) + u(n). \tag{6}$$

In the specific framework of ultrasound NDT, the first term of $s(n)$, i.e. $w(n)$, corresponds to front side reflection, while the $(Q-1)$ subsequent terms are associated to reflections on defects. This model applies when, as compared to the front side echo, the defect echos have the same shape and are attenuated by factors defined by a_i and delayed by n_i samples. Moreover, provided the defects are situated deeply enough in the considered material sample, the associated $(Q-1)$ terms in (6) have no temporal overlap with the term $w(n)$ corresponding to front side reflection. Therefore, when measuring $s(n)$, the signal $w(n)$ is also available: it is extracted as the beginning of the overall recorded signal $s(n)$, and then zero padded so that both signals have the same number N of samples. We then consider the Fourier Transforms (FT) of these signals, at discrete frequencies

$$f = \frac{k}{N}, \tag{7}$$

where k is an integer. These FT values may be considered as values of functions of k and are therefore denoted $W(k)$ and $S(k)$ hereafter. Taking the FT of (6) then yields

$$S(k) = W(k) + \sum_{i=2}^{Q} a_i e^{-j2\pi k \frac{n_i}{N}} W(k) + U(k). \tag{8}$$

Let us then define the signal[1]

$$X(k) = \frac{S(k)}{W(k)} - 1. \tag{9}$$

Eq. (8) yields

$$X(k) = \sum_{i=2}^{Q} a_i e^{-j2\pi k \frac{n_i}{N}} + V(k) \tag{10}$$

with

$$V(k) = \frac{U(k)}{W(k)}. \tag{11}$$

As shown by (10), the signal $X(k)$ thus turns out to be a sum of complex sinusoids and of noise $V(k)$. Let us stress that $X(k)$ is a *frequency-domain* process, i.e. a function of the integer k which is linked to the frequency f by (7). The "frequencies", in the corresponding temporal space, of the considered sinusoids are the unknown parameters $-\frac{n_i}{N}$.

Our initial problem, i.e. the estimation of the time delays n_i, is thus reformulated in the same way as the standard spectral analysis problem that we described above, except that the time and frequency domains have been permuted, i.e. the analyzed process $X(k)$ is defined in the frequency domain instead of the time domain. This estimation problem may therefore be solved by using the above-defined high-resolution methods, taking into account the above time/frequency permutation (and provided the noise component meets the requirements of these methods). It should be noted that this general approach has also been used for 2-D signals [6], in order to estimate spatial shifts in images by using an extended MUSIC-based method.

In our 1-D case, the practical methods which result from the above principles may be defined as follows. The vector of exponentials (4) here becomes (see its 2-D version in [6])

$$\epsilon = [1 \quad exp\ (-j2\pi\frac{n}{N}) \quad \dots \quad exp\ (-j2\pi(L-1)\frac{n}{N})]^T \tag{12}$$

and the functions (3) and (5) to be maximized are

$$\hat{T}_{MV}(n) = \frac{1}{\epsilon^H \hat{R}_{XX}^{-1} \epsilon} \tag{13}$$

and

$$\hat{T}_{MUSIC}(n) = \frac{1}{\sum_{i=Q+1}^{L} |\epsilon^H \hat{v}_i|^2} \tag{14}$$

where the vectors $\hat{v}_i$ are defined in the same way as above, but now with respect to the estimated autocorrelation matrix $\hat{R}_{XX}$ of the frequency-domain process $X(k)$. The entry with indices (p, q) of the autocorrelation matrix R_{XX} reads

$$E\{X(k+p)X^*(k+q)\} \quad \forall\ k, \quad 0 \le p \le L-1, \quad 0 \le q \le L-1 \tag{15}$$

where $E\{\}$ stands for expectation.

The last issue to be addressed is therefore how to estimate these expected values. In the classical signal processing methods which concern time-domain random processes, expectations are estimated by considering temporal means associated to the time samples of the considered signal $x(n)$, based on ergodicity assumptions [4]. If we assume that the same approach[2] may here be applied to the frequency-domain process $X(k)$, then each

[1] Equivalently, one may use instead of $s(n)$ a modified version of this signal, where its beginning is reset to 0 in order to remove the component $w(n)$ initially contained by $s(n)$. The first term $W(k)$ is then removed from (8), so that the term "- 1" is not introduced in (9).

[2] An alternative approach may be defined as follows in application domains where the initial time-domain signals contain enough samples. These signals are first split in several windows. Discrete Fourier Transforms (DFTs) are then independently computed for each window and the means of these DFTs over all windows are then used to derive estimates of the above expectations. The 2-D version of this approach is e.g. used in [6].

entry (15) of the estimated autocorrelation matrix $\hat{R}_{XX}$ is obtained as the sample mean of $X(k+p)X^*(k+q)$, where this mean is computed over the frequencies associated to values of k, defined in (7). This sample mean reads explicitly

$$\frac{1}{N}\sum_{k=0}^{N-1} X(k+p)X^*(k+q) \tag{16}$$

where $X(k)$ is a periodic function of k with period N. The resulting overall matrix $\hat{R}_{XX}$ may then be expressed as

$$\hat{R}_{XX} = \frac{1}{N}\sum_{k=0}^{N-1} V_X(k)V_X(k)^H \tag{17}$$

with

$$V_X(k) = [X(k), \ldots, X(k+L-1)]^T. \tag{18}$$

It should be noted that this final expression of these high-resolution TDE approaches was provided, also in the frame of NDT, in [7], without explicit proofs but with a reference to [8].

3 Filter identification method

We now consider the situation when two real-valued signals $x(n)$ and $y(n)$ are available, and $y(n)$ is a filtered version of $x(n)$, through a causal L-th order Finite Impulse Response (FIR) filter. We aim at estimating the real-valued coefficients $h(n)$ of the impulse response of this filter, with $0 \leq n \leq L-1$. The frequency response of this filter is the Fourier Transform (FT) of its impulse response, i.e[3]

$$H(\omega) = \sum_{n=0}^{L-1} h(n)e^{-j\omega n}. \tag{19}$$

In this equation, the coefficients $h(n)$ are unknown, while an estimate $\hat{H}(\omega)$ of $H(\omega)$ may be derived, e.g. as the ratio of the FTs of the available signals $x(n)$ and $y(n)$, or by using more advanced methods. If we now use this estimate in (19) and consider the real and imaginary parts of this equation, taking into account that the coefficients $h(n)$ are real-valued, we obtain (up to estimation errors)

$$\sum_{n=0}^{L-1} h(n)cos(\omega n) = Re(\hat{H}(\omega)) \tag{20}$$

$$\sum_{n=0}^{L-1} -h(n)sin(\omega n) = Im(\hat{H}(\omega)) \tag{21}$$

which yields two equations with unknown $h(n)$. Moreover, these equations hold for any angular frequency ω. Let us now apply this principle to a set of P angular frequencies $\omega_1 \ldots \omega_P$, which may especially correspond to Discrete Fourier Transforms (DFTs). Eq. (20)- (21) then yield a set of $2P$ equations, which may be expressed in matrix form as

$$Mv_h = v_{\hat{H}} \tag{22}$$

with

$$v_h = [h(0), \ldots, h(L-1)]^T \tag{23}$$

$$M = \begin{bmatrix} 1 & cos[\omega_1] & \ldots & cos[(L-1)\omega_1] \\ \ldots & \ldots & \ldots & \ldots \\ 1 & cos[\omega_P] & \ldots & cos[(L-1)\omega_P] \\ 0 & -sin[\omega_1] & \ldots & -sin[(L-1)\omega_1] \\ \ldots & \ldots & \ldots & \ldots \\ 0 & -sin[\omega_P] & \ldots & -sin[(L-1)\omega_P] \end{bmatrix} \tag{24}$$

$$v_{\hat{H}} = [Re(\hat{H}(\omega_1)), \ldots, Re(\hat{H}(\omega_P)), Im(\hat{H}(\omega_1)), \ldots, Im(\hat{H}(\omega_P))]^T. \tag{25}$$

[3]Unlike in Section 2, FTs are here considered as functions of the angular frequency ω. They are denoted in the same way as in Section 2 however, for the sake of simplicity.

Provided the number of selected angular frequencies is large enough to have $2P \geq L$, the linear set of equations (22) may then be inverted, e.g. using Moore-Penrose pseudo-inverse. This yields the impulse response coefficients $h(n)$ which form v_h.

Provided the filter order L is small enough, this identification method only requires the frequency response of this filter to be estimated at a few frequencies. It is therefore e.g. of interest for relatively narrow-band signals (such as ultrasound NDT signals) because they only yield accurate estimates $\hat{H}(\omega)$ in their restricted band, which corresponds to a few DFT frequencies.

This generic method is applied in the same way as in Section 2 to the ultrasound NDT signal, which is here defined by (2) however, i.e.

- the input signal $x(n)$ of this identification method is then the front side reflection signal $w(n)$, which is again extracted as the beginning of the overall A-SCAN signal $s(n)$, still assuming that the front side and defect signals have no temporal overlap,
- the output signal $y(n)$ is the defect reflection signal $w(n) * h(n)$ in (2), which is extracted as the end of the overall A-SCAN signal $s(n)$.

We developed this approach independently, but it should be noted that similar methods were also reported in the literature (see e.g. the survey in [9]).

4 Experimental results and conclusions

The performance of the MV and MUSIC time-delay estimation methods was first tested with signals obtained as follows. A real front-side echo was used as the signal $w(n)$. An artificial A-SCAN signal $s(n)$ was then derived from it according to the model (1), with $a = 0.5$ and $n_0 = 278$. This overall signal is shown in Fig. 1 (a), while Fig. 1 (b) and (c) contain the experimental functions $\hat{T}_{MUSIC}(n)$ and $\hat{T}_{MV}(n)$, computed with $L = 20$. As explained above, the sample indices n associated to the maxima of these functions are the estimated values $\hat{n}_0$ of the delay parameter n_0. Fig. 1 (b) and (c) then show that both methods estimate n_0 very accurately. More precisely, zoomed versions of these figures show that both methods yield $\hat{n}_0 = 279 = n_0 + 1$.

The same approach was then applied to a real A-SCAN signal recorded from a sample of polystyrene, where the "defect echo" actually corresponds to the reflection on the back side of the sample. Fig. 2 (a) shows that the two echos have similar shapes (with a phase reversal, i.e. $a < 0$ in (1)). The model (1) is therefore quite relevant for this real signal. However, the actual delay n_0 is here unknown. It is considered to be equal to the delay between the corresponding extrema of the two echos, i.e. $n_0 = 378$. Fig. 2 (b) and (c) then show that the MUSIC and MV methods here again estimate this delay very accurately, i.e. they resp. yield $\hat{n}_0 = 381$ and $\hat{n}_0 = 379$.

This approach was eventually applied to a sample of Titanium Aluminide (TiAl), with a defect consisting of a flat bottom hole. Fig. 3 shows that, although the echos have somewhat different waveforms, their delay $n_0 = 333$ is relatively accurately estimated: the functions $\hat{T}_{MUSIC}(n)$ and $\hat{T}_{MV}(n)$ of the considered methods still contain a single, sharp, peak and they resp. yield $\hat{n}_0 = 321$ and $\hat{n}_0 = 319$.

The performance of the filter identification method described in Section 3 was then tested with a signal created according to (2), where $w(n)$ is again a real recorded echo and $h(n)$ was set as follows (up to a time delay n_1 which is omitted below for better readability): $h(n) = 1$ if $1 \leq n \leq 10$ and $h(n) = 0$ otherwise. Fig. 4 (a) contains the resulting A-SCAN signal (with normalized echo magnitude for better readability). Fig 4 (b) shows that the considered method (here applied with L= 51) succeeds in estimating $h(n)$ very accurately.

As a conclusion, the tests performed so far demonstrate the good performance of the proposed methods in the considered conditions. The next stage of this investigation will mainly consist in applying the above identification method to real signals, such as those recorded from polystyrene and TiAl samples, in order to estimate and interpret the corresponding impulse responses $h(n)$.

References

[1] J. Capon, "High-resolution frequency-wavenumber spectrum analysis", Proceedings of the IEEE, vol. 57, no. 8, pp. 1408-1418, Aug. 1969.

[2] R. Schmidt, "Multiple emitter location and signal parameter estimation", Proceedings of the RADC Spectral Estimation Workshop, pp. 243-258, Rome, NY 1979.

[3] D. H. Johnson, D. E. Dudgeon, Array Signal Processing: Concepts and Techniques, Prentice Hall, Englewood Cliffs, NJ 07632, 1993.

[4] S. M. Kay, "Modern spectral estimation. Theory & application", Prentice Hall, Englewood Cliffs, New Jersey, 1988.
[5] S.M. Kay, S.L. Marple, "Spectrum analysis - a modern perspective", Proceedings of the IEEE, vol. 69, no. 11, pp. 1380-1419, Nov. 1981.
[6] M. Gunsay, B. D. Jeffs, "Point-source localization in blurred images by a frequency-domain eigenvector-based method", IEEE Transactions on Image Processing, vol. 4, no. 12, Dec. 1995.
[7] M. Boulouz, E. Gonneau, J.P. Guilhot, "Comparaison d'algorithmes de détection en contrôle non destructif, 5e Congrès Français d'Acoustique, 3-6 Sept. 2000, Lausanne, Suisse.
[8] A. Ouamri, "Etude des performances des méthodes d'identification à haute résolution et application à l'identification des échos par une antenne linéaire multicapteur", Thèse de Doctorat, Université Paris XI, France, 1986.
[9] E. Balmès, "Methods for vibration design and validation", report from Ecole Centrale Paris, Chatenay Malabry, France, 2005. Available at http://www.sdtools.com/pdf/PolyId.pdf

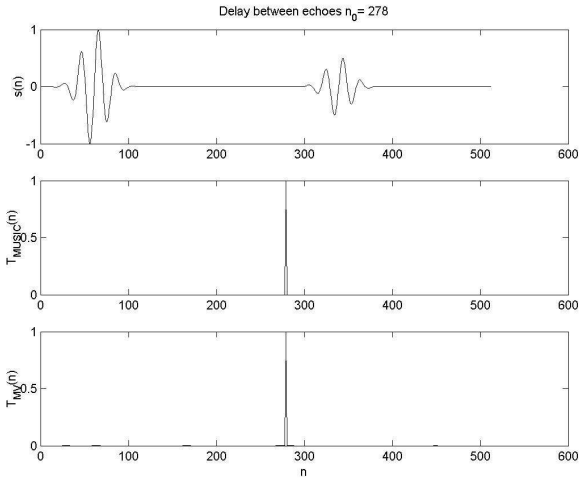

Fig. 1

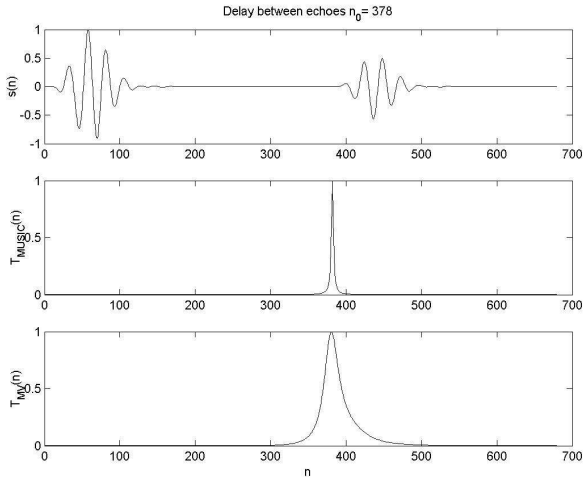

Fig. 2

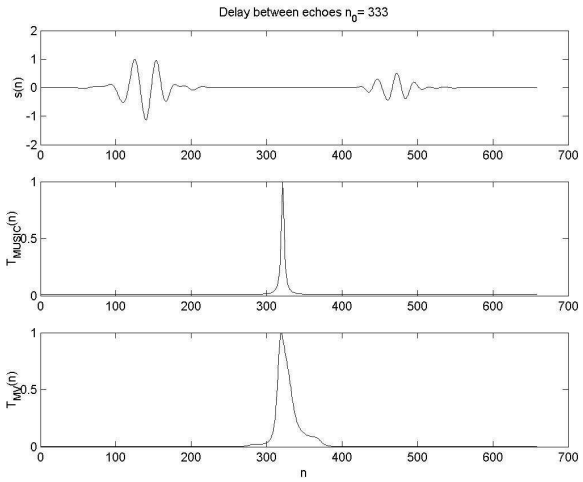

Fig. 3

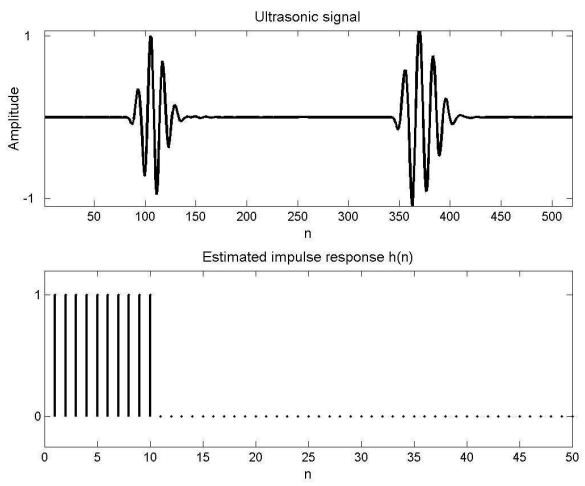

Fig. 4

Fig. 1 to 3: (a) A-SCAN signal (top), (b) $\hat{T}_{MUSIC}(n)$ (middle) and (c) $\hat{T}_{MV}(n)$ (bottom), resp. for synthetic signal, polystyrene and TiAl samples.
Fig. 4: (a) A-SCAN signal (top), (b) estimated impulse response (bottom).